



Synthesis, Characterization, X-ray Diffraction Studies, and Biological Evaluation of Tert-butyl 4-(5-(3-fluorophenyl)-1,2,4-oxadiazol-3-yl) piperazine-1-carboxylate

C. Sanjeevarayappa, Pushpa Iyengar, K. E. Manoj Kumar & P. A. Suchetan

To cite this article: C. Sanjeevarayappa, Pushpa Iyengar, K. E. Manoj Kumar & P. A. Suchetan (2015) Synthesis, Characterization, X-ray Diffraction Studies, and Biological Evaluation of Tert-butyl 4-(5-(3-fluorophenyl)-1,2,4-oxadiazol-3-yl) piperazine-1-carboxylate, Molecular Crystals and Liquid Crystals, 607:1, 232-241, DOI: [10.1080/15421406.2014.928979](https://doi.org/10.1080/15421406.2014.928979)

To link to this article: <http://dx.doi.org/10.1080/15421406.2014.928979>



Published online: 26 Feb 2015.



Submit your article to this journal [↗](#)



Article views: 28



View related articles [↗](#)



View Crossmark data [↗](#)

Synthesis, Characterization, X-ray Diffraction Studies, and Biological Evaluation of Tert-butyl 4-(5-(3-fluorophenyl)-1,2,4-oxadiazol-3-yl) piperazine-1-carboxylate

C. SANJEEVARAYAPPA,¹ PUSHPA IYENGAR,¹ K. E. MANOJ KUMAR,² AND P. A. SUCHETAN^{3,*}

¹East Point Research Academy, Bidarahalli, Bangalore & GFGC, Yelahanka, Bangalore, India

²Department of Chemistry, KLE's S N College, Bangalore, Karnataka, India

³Department of Chemistry, UCS, Tumkur University, Tumkur, Karnataka, India

*The title compound tert-butyl 4-(5-(3-fluorophenyl)-1,2,4-oxadiazol-3-yl)piperazine-1-carboxylate was synthesized by condensation reaction between carbamimide and 3-fluorobenzoic acid in the presence of 3-(3-dimethylaminopropyl)carbodiimide hydrochloride and hydroxybenzotriazole under basic condition. It was characterized by spectroscopic evidences such as LCMS, ¹H NMR, ¹³C NMR, IR, and CHN elemental analysis. The structure was further confirmed by single crystal XRD data. The title compound, C₁₇H₂₁FN₄O₃, crystallized in the monoclinic crystal system and P2₁/c space group with the unit cell parameters $a = 14.281(3) \text{ \AA}$, $b = 11.579(2) \text{ \AA}$, $c = 11.331(2) \text{ \AA}$, $\beta = 110.674(6)^\circ$, $Z = 4$, and $V = 1753.0(6) \text{ \AA}^3$. In the structure, the molecules are linked through weak C—H...O intermolecular interactions along [010], and aromatic π – π stacking interactions (centroid-centroid distance = $3.7456(15) \text{ \AA}$) generate a three-dimensional architecture. The compound was screened for its *in vitro* antibacterial and anthelmintic activity. The compound exhibited poor antibacterial and moderate anthelmintic activity.*

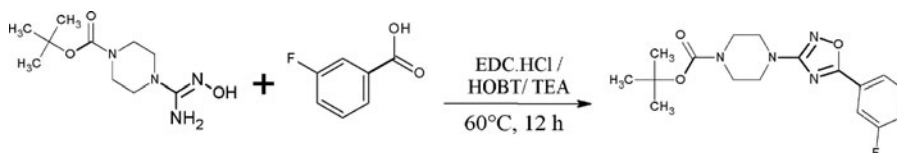
Keywords 1,2,4-oxadiazole; anthelmintic activity; antibacterial activity; XRD

Introduction

1,2,4-Oxadiazoles are known for their diverse biological activities [1]. They have been described as bio-isosteres for amides and esters. Oxadiazole ring, due to their better hydrolytic and metabolic stabilities, improved pharmacokinetic, and *in vivo* performance are often observed, which makes them an important structural moiety for the pharmaceutical industry [2]. As a result of these, oxadiazoles have often been the target of numerous drug discovery programs as anti-inflammatory agents, antitumor agents, potential anticancer agents, Histamine H₃ receptor antagonists as potent inhibitors of MIF biological function, and bell-tryptase inhibitors. In addition to these, 1,2,4-oxadiazoles are widely used as

*Address correspondence to P. A. Suchetan, Department of Chemistry, UCS, Tumkur University, Tumkur, Karnataka - 572103, India. E-mail: pasuchetan@yahoo.co.in

Color versions of one or more of the figures in the article can be found online at www.tandfonline.com/gmcl.



Scheme 1.

hydrolysis resisting amide bioisosteres in the development of peptidomimetics [3]. Also, oxadiazoles exhibit a wide range of antibacterial, antifungal and activities against Gram-positive and Gram-negative bacteria. Further, acid amide containing oxadiazole nucleus and their derivatives were evaluated for a variety of pharmacological activities such as anti-tubercular [4], antiallergic [5], anti-inflammatory [6], central nervous system depressant activity [7], and ulcerogenic activity [8]. In view of these pharmacological positive results in literature survey, we planned to synthesize new series of amides bearing 1,2,4-oxadiazole nucleus and evaluated their antimicrobial and anthelmintic potential.

Materials and Methods

Melting point was determined in open capillary and is uncorrected. The molecular structure of the synthesized compound was established using IR, ^1H NMR, ^{13}C NMR, and LC-MS data. FT-IR Spectra was recorded on Jasco FT-IR Spectrometer, ^1H NMR and ^{13}C NMR were recorded in CDCl_3 at 399.65 and 100.50 MHz, respectively, on Bruker model avance II. All the chemical shifts were reported in parts per million (ppm) using tetramethylsilane as an internal standard. LC-MS was recorded using Waters Alliance 2795 separations module and Waters Micromass LCT mass detector. Elemental analysis (C, H, and N) was performed on an Elementar vario MICRO cube. The purity of the compound was confirmed using Thin-Layer Chromatography (TLC) on precoated silica gel plate and further purification was done using column chromatography. Single crystal X-ray diffraction studies were carried out in Bruker Smart X2S diffractometer.

Experimental Section

Synthesis of tert-butyl 4-[5-(3-fluorophenyl)-1,2,4-oxadiazol-3-yl]piperazine-1-carboxylate

The title compound was synthesized according to the known procedure reported in literature [9] (Scheme 1). 3-Fluorobenzoic acid (0.08 mol, 16.8 g), hydroxybenzotriazole (0.01 mol, 0.1 g), and 3-(3-dimethylaminopropyl)carbodiimide hydrochloride (0.128 mol, 20.75 g) were taken in 200 mL methylene dichloride. The reaction mixture was stirred for half an hour at room temperature in a 500 mL round bottomed flask. To this mixture, tert-butyl-4-(N'-hydroxycarbonylmethyl) piperazine-1-carboxylate (0.08 mol, 20 g) was added and the reaction mixture was stirred at 60°C for 12 h. The reaction was monitored by TLC. Methylene dichloride was distilled off and the residue was poured into vigorously stirred ice-cold water, the pale yellow solid thus obtained was collected by filtration. Crude product was purified by column chromatography using petroleum ether/ethyl acetate as eluent (7:3). Pale yellow colored solid was recrystallized by petroleum ether and ethyl acetate (8:2) solvent system (Yield 38%, MP: $198\text{--}199^\circ\text{C}$).

Table 1. Crystal data and structure refinement

CCDC number	CCDC 949436
Empirical formula	C ₁₇ H ₂₁ FN ₄ O ₃
Formula weight	348.38
Temperature/K	99(2)
Crystal system	monoclinic
Space group	P2 ₁ /c
a/Å	14.281(3)
b/Å	11.579(2)
c/Å	11.331(2)
$\beta/^\circ$	110.674(6)
Volume/Å ³	1753.0(6)
Z	4
ρ_{calc} mg/mm ³	1.320
Absorption coefficient	0.099
<i>F</i> (000)	736.0
Crystal size/mm ³	0.32 × 0.27 × 0.24
2 θ range for data collection	4.66 to 48.5°
Index ranges	−15 ≤ <i>h</i> ≤ 16, −10 ≤ <i>k</i> ≤ 13, −13 ≤ <i>l</i> ≤ 7
Reflections collected	10768
Independent reflections	2755 [<i>R</i> (int) = 0.1014]
Data/restraints/parameters	2755/2/233
Goodness-of-fit on <i>F</i> ²	1.078
Final <i>R</i> indexes [<i>I</i> > = 2 σ (<i>I</i>)]	<i>R</i> ₁ = 0.0466, <i>wR</i> ₂ = 0.1177
Final <i>R</i> indexes [all data]	<i>R</i> ₁ = 0.0720, <i>wR</i> ₂ = 0.1341
Largest diff. peak/hole/eÅ ^{−3}	0.19/−0.28

Crystal Structure Determination

Colorless prisms of the compound were obtained from slow evaporation of the solution of the compound in a mixture of pet ether and ethyl acetate (1:2).

A colorless prism of the title compound with dimensions 0.32 × 0.27 × 0.24 mm was chosen for X-ray diffraction study. The data were collected on a Bruker Smart X2S diffractometer equipped with a fine focus, 3 kW sealed X-ray source (graphite monochromated Mo *K*α). The crystal to detector distance was fixed at 120 mm with a detector area of 422 × 221 mm². Thirty six frames of data were collected at room temperature by the oscillation method. Each exposure of the image plate was set to a period of 300 s. Successive frames were scanned in steps of 5°/min with an oscillation range of 5°. Image processing and data reduction were done using SAINT-Plus and XPREP [10]. All the frames could be indexed using a primitive monoclinic lattice. The structure was solved by direct methods using SHELXS-97 [11]. All the Q peaks of non-hydrogen atoms were located in the first Fourier map itself. Full-matrix least squares refinement using SHELXL-97 [11] with isotropic temperature factors for all the atoms converged the residuals to *R*₁ = 0.101. In the second stage, nonhydrogen atoms were refined anisotropically. All H atoms were positioned geometrically, with C–H = 0.95 Å for aromatic H, C–H = 0.99 Å for methylene H, and C–H = 0.98 Å for methyl H, and refined using a riding model with *U*_{iso}(H) = 1.5 *U*_{eq}(C) for methyl H and *U*_{iso}(H) = 1.2 *U*_{eq}(C) for all other H. The C–F

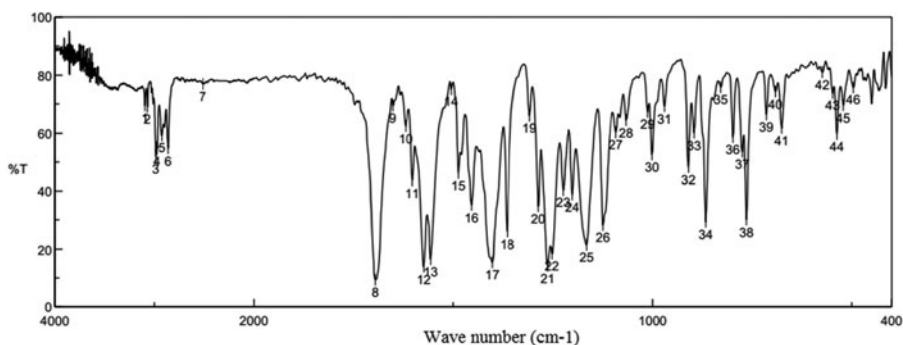


Figure 1. Infrared spectrum of the synthesized compound.

bonds in both the major and minor components were fixed to 1.340(1) [12]. The minor component F atom was given the same anisotropic thermal parameter as that of the major component. These positions were checked on a final difference map and were found to be satisfactory. 233 parameters were refined with 2,755 unique reflections which saturated the residuals to $R_1 = 0.0466$. The details of the crystal data and refinement are given in Table 1.

Results and Discussion

The compound was synthesized according to the Scheme 1 and characterized by elemental analysis (C, H, N), LC-MS, IR, ^1H and ^{13}C NMR, and single crystal X-ray diffraction

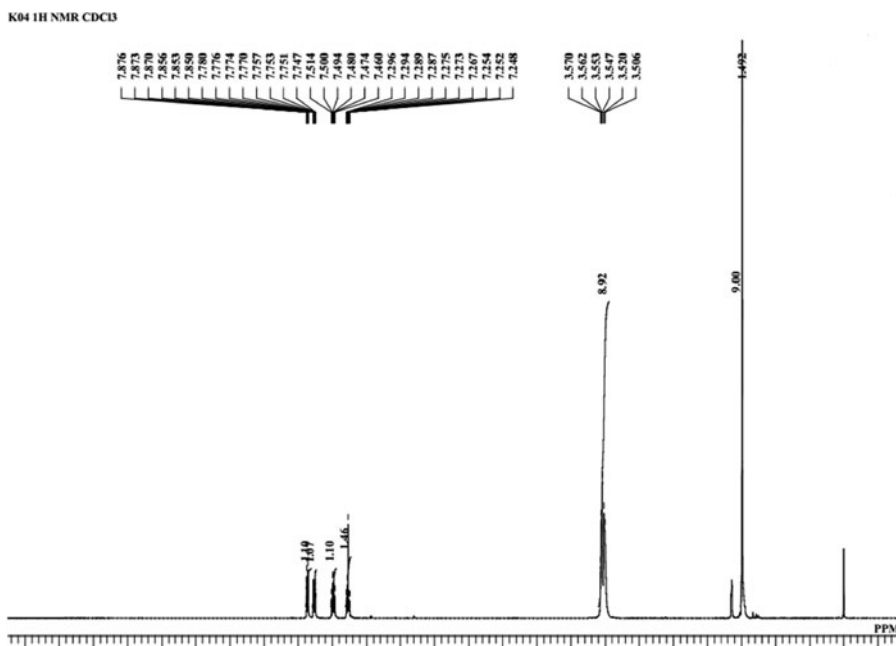


Figure 2. ^1H NMR spectrum of the synthesized compound.

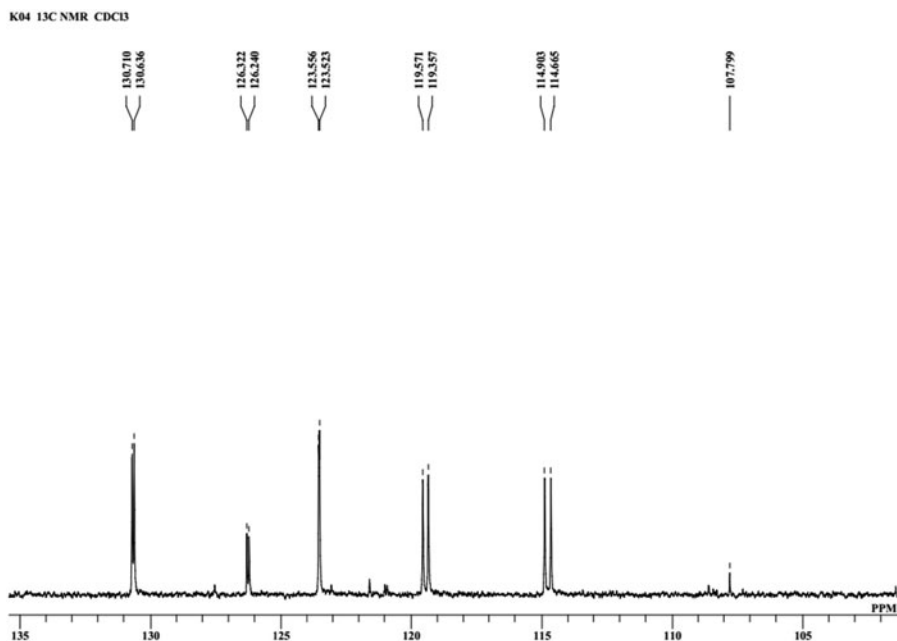


Figure 3. ^{13}C NMR spectrum of the synthesized compound.

studies. Spectral data of the synthesized compound is in full agreement with its proposed structure. In the IR spectrum (Fig. 1), absorption bands at 2983.34 and 2970.8 cm^{-1} are due to aliphatic CH groups, bands at 1696 cm^{-1} due to $\text{C}=\text{O}$ group, 1573 cm^{-1} due to $\text{C}-\text{O}$ stretching and bands at $1402\text{--}1364\text{ cm}^{-1}$ due to $\text{C}-\text{F}$ stretching. In the ^1H NMR (Fig. 2) spectrum, the signals of the respective protons of the title compound are verified on the basis of their chemical shifts, multiplicities, and coupling constants and are as follows.

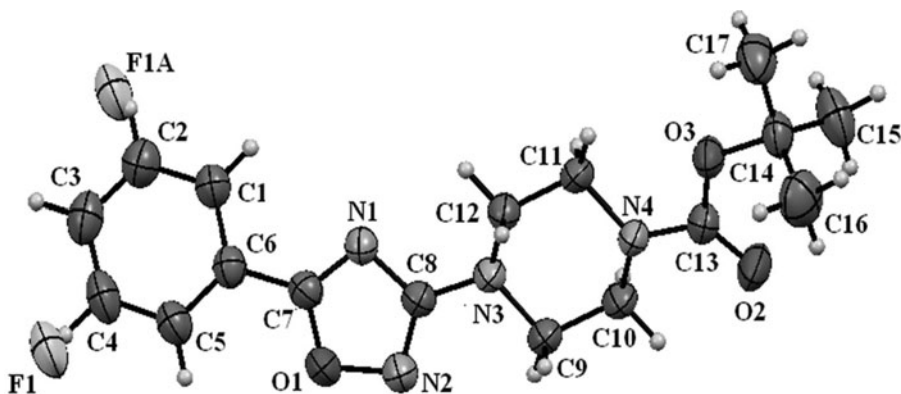


Figure 4. Molecular structure of the title compound, showing displacement ellipsoids drawn at the 50% probability level.

Table 2. Bond lengths

Bond	Length (Å)	Bond	Length (Å)
O1-N2	1.434(2)	C1-C2	1.375(3)
O1-C7	1.348(2)	C1-C6	1.391(3)
O2-C13	1.219(2)	C2-F1A	1.3390(11)
O3-C13	1.343(2)	C2-C3	1.370(3)
O3-C14	1.472(2)	C3-C4	1.371(3)
N1-C7	1.294(3)	C4-F1	1.3398(10)
N1-C8	1.383(3)	C4-C5	1.372(3)
N2-C8	1.313(3)	C5-C6	1.389(3)
N3-C8	1.369(3)	C6-C7	1.460(3)
N3-C9	1.460(2)	C9-C10	1.518(3)
N3-C12	1.465(3)	C11-C12	1.509(3)
N4-C10	1.459(3)	C14-C15	1.520(3)
N4-C11	1.469(2)	C14-C16	1.514(3)
N4-C13	1.360(3)	C14-C17	1.516(3)

$^1\text{H-NMR}$ (CDCl_3) δ ppm: 7.87 (d, $J = 7.9$ Hz, 1H, Ar-H), 7.78 (dd, $J = 2.39$ and $J = 9.19$, 1H, Ar-H) 7.51 (m, 1H, Ar-H), 7.29 (m, 1H, Ar-H), 3.57 (t, $J = 6.7$ Hz, 8 H, $(\text{H}_2\text{C-N-CH}_2)_2$), 1.49 (s, 9H, 3CH_3).

The ^{13}C NMR spectrum (Fig. 3) shows peak at $\delta = 173.28$ ppm for a carbonyl carbon. The signals due to other carbon atoms are as follows:

Table 3. Bond angles

Bond	Angle (°)	Bond	Angle (°)
C7-O1-N2	106.20(15)	C5-C6-C7	121.5(2)
C13-O3-C14	121.71(16)	O1-C7-C6	117.82(18)
C7-N1-C8	102.75(17)	N1-C7-O1	113.59(18)
C8-N2-O1	102.40(16)	N1-C7-C6	128.6(2)
C8-N3-C9	116.77(16)	N2-C8-N1	115.01(18)
C8-N3-C12	117.28(16)	N2-C8-N3	123.21(18)
C9-N3-C12	113.95(16)	N3-C8-N1	121.73(18)
C10-N4-C11	112.96(16)	N3-C9-C10	110.16(17)
C13-N4-C10	118.32(16)	N4-C10-C9	110.88(16)
C13-N4-C11	122.62(17)	N4-C11-C12	109.90(17)
C2-C1-C6	119.6(2)	N3-C12-C11	110.32(17)
F1A-C2-C1	128.7(6)	O2-C13-O3	124.9(2)
F1A-C2-C3	109.0(5)	O2-C13-N4	123.6(2)
C3-C2-C1	121.4(2)	O3-C13-N4	111.51(17)
C4-C3-C2	118.0(2)	O3-C14-C15	110.43(18)
C3-C4-C5	122.93(18)	O3-C14-C16	109.86(18)
F1-C4-C3	117.5(2)	O3-C14-C17	102.18(17)
F1-C4-C5	119.5(2)	C16-C14-C15	112.6(2)
C4-C5-C6	118.3(2)	C16-C14-C17	111.1(2)
C1-C6-C7	118.8(2)	C17-C14-C15	110.2(2)
C5-C6-C1	119.8(2)		

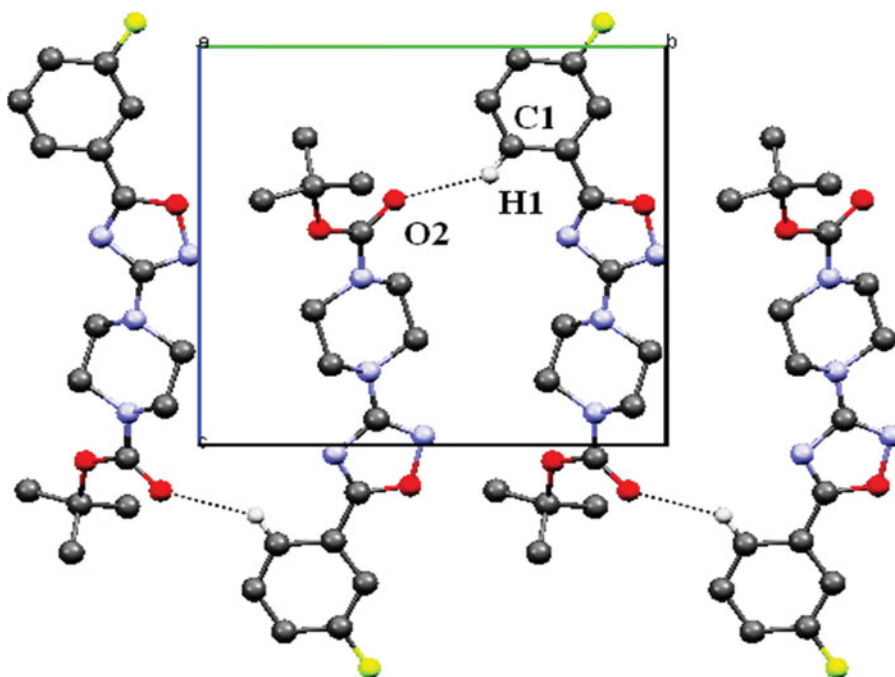


Figure 5. Molecular packing into C(12) chains along [010] when viewed down the *a* axis. H atoms not involved in H-bonding are omitted for clarity.

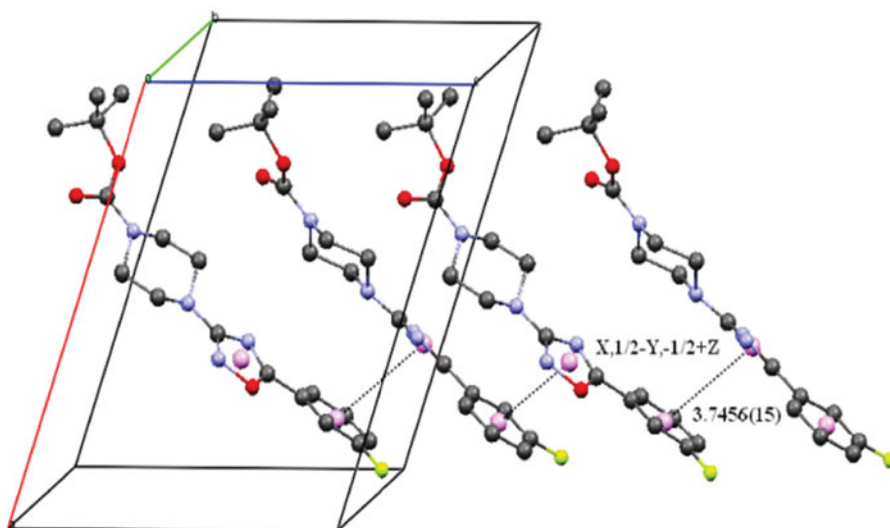


Figure 6. π - π stacking interactions along *c* axis between the fluorobenzene and the oxadiazole ring. H atoms are omitted for clarity.

Table 4. Hydrogen bond geometry (Å, deg)

D-H... A	d(D-H)	d(H-A)	d(D-A)	D-H-A
C1-H1... O2 [#]	0.95	2.51	3.252(3)	134.9

[#]1-X, -1/2+Y, 3/2-Z.

¹³C-NMR (CDCl₃): δ ppm: 173.2 (C=O), 170.2 (N-C-N), 163.8 (N-C-O), 161.3 (ipso carbon), 154.5 (C-F), 130.7 (Ar-C), 123.5 (Ar-C), 119.5 (Ar-C), 114.9 (Ar-C), 80.0 (O-C(CH₃)), 45.7 (2C, N-(CH₂)₂), 43.1 (2C, Nbond;(CH₂)₂), 28.2 (3C, (CH₃)₃).

The mass spectrum shows the presence of a peak at m/z 349.3 (M+1) in accordance with the molecular formula. Elemental analysis also gives satisfactory results for the title compound [Calc (Found): C, 58.61% (58.58%); H, 6.08% (6.04%); N, 16.08% (16.02%)].

Molecular and Crystal Structure

The structure of the molecule [13] with thermal ellipsoids drawn at 50% probability is shown in Fig. 4. Tables 2 and 3 gives the list of bond distances and bond angles of nonhydrogen atoms, respectively. The bond lengths and bond angles are in good agreement with the standard values. The compound, crystallizes in the monoclinic crystal system and $P2_1/c$ space group with the unit cell parameters $a = 14.281(3)$ Å, $b = 11.579(2)$ Å, $c = 11.331(2)$ Å, $\beta = 110.674(6)^\circ$, $Z = 4$, and $V = 1753.0(6)$ Å³. The piperazine ring in the structure adopts chair conformation, which is confirmed by the puckering amplitude $Q = 0.545(2)$ Å, and angles $\theta = 179.6(2)^\circ$ and $\Phi = 46.0(7)^\circ$. Further, the bonds N3-C8 and N4-C13 make an angle $89.52(15)^\circ$ and $79.09(15)^\circ$, respectively, with the Cremer and Pople (C & P) plane [14] of the piperazine ring, and thus are in the equatorial plane of the piperazine ring. In the molecule, the best fit plane through all the nonhydrogen atoms of the piperazine ring forms dihedral angles of $31.95(11)^\circ$ and $16.61(12)^\circ$, respectively, with the oxadiazole and the fluorobenzene ring. Further, the dihedral angle between the oxadiazole and the fluorobenzene ring is $17.57(12)^\circ$. The fluorophenyl ring is disordered over two orientations with occupancies of 0.877 (3) and 0.123 (3).

In the crystal structure, the molecules are linked into C(12) chains [15] through a weak C1-H1...O2 interaction along [010]. π - π stacking interactions between the fluorobenzene and the oxadiazole ring are also observed in the crystal structure. The angle between the planes in the π - π stacking is $12.52(12)^\circ$, the centroid-centroid separation is $3.7456(15)$ Å and the perpendicular distance between the planes defining the two rings is $3.3463(9)$ Å. The packing of molecules through C-H...O and π - π stacking interactions are respectively shown in Figs. 5 and 6. The hydrogen bond parameters are given in Table 4.

Table 5. Antibacterial activity of compound

Compound	<i>S. aureus</i>	<i>S. citreus</i>	<i>B. polymyxa</i>	<i>B. cereus</i>
Our compound	00	17	14	14
CIPX	28	27	24	24

CIPX = Ciprofloxacin is used as a positive control, and the zone of inhibition is expressed in mm.

Table 6. Anthelmintic activity of compound against *Pheretima posthuma*

Test samples	Concentration (mg/ml)	Time taken for paralysis (min)	Time taken for death (min)
Control	–	142.33 ± 0.49	167.17 ± 0.87
Piperazine citrate	50	39.17 ± 0.48**	57.00 ± 0.58**
Our compound	100	38.00 ± 1.59	58.50 ± 0.76
	50	68.00 ± 1.46**	108.00 ± 0.86**

Values are the mean ± SEM of three earthworms. Symbols represent statistical significance * $p < 0.05$, ** $p < 0.01$, ns: not significant as compared to control group.

Antibacterial Activity

The synthesized compound was screened for their antibacterial activity. Different concentrations of test compound were prepared using DMSO and tested against *Staphylococcus aureus*, *Staphylococcus citreus*, *Bacillus polymyx*, and *Bacillus cereus* bacterial stains by disc diffusion method [16, 17] using ciprofloxacin (5 µg/50 µL) as standard. The disks with 6.0 mm in diameter were prepared using filter paper. Disks were kept in screw capped bottle and sterilized at 140°C for 1 h. Disk for the experiment was prepared by taking twice the amount of test compounds solution required for each disc and added to bottle containing disks. Disks with different concentration of test compounds were placed on the nutrient agar media in two sets on fresh bacteria seeded on agar media and incubated for 12 h at 35°C. The minimum inhibitory concentration was noted by observing the lowest concentration of the drug which resulted in inhibition of bacterial growth. Title compound showed poor antibacterial property. Results are tabulated in Table 5.

Anthelmintic Activity

Anthelmintic activity of the compound was done by using *Pheretima posthuma* (Indian Earthworm). Worms were maintained under normal vermicomposting medium with adequate supply of nourishment and water for about 3 weeks. Adult earthworms of approximately 4 cm in length and 0.2–0.3 cm in width were chosen for the experiment. Different concentrations of 50 and 100 mg samples were evaluated as per the standard method reported [18]. Five groups of each with six earth worms were taken. Each *P. posthuma* was washed separately with normal saline before the initiation of experimental procedure and placed into a 20 ml of normal saline. Group I earthworms were placed in 20 ml saline in a clean Petri plate and Group II earthworms were placed in 20 ml saline containing standard drug piperazine citrate (50 mg/ml). Similarly, Group III–XI earthworms were placed in a 20 ml saline containing 50 and 100 mg/ml of test samples respectively. Observation was done keeping time taken for paralysis and the time taken for death as objective and was documented in minutes. Paralysis time was analyzed based on behavior of the worms with no revival body state in normal saline medium. Death was concluded based on total loss of motility with faded body color and the results are illustrated in Table 6.

Conclusion

A 1,2,4-oxadiazole derivative, tert-butyl 4-(5-(3-fluorophenyl)-1,2,4-oxadiazol-3-yl)piperazine-1-carboxylate, was synthesized and well characterized by IR, ^1H NMR, ^{13}C NMR,

LCMS, and single crystal XRD data. The compound was screened for its in vitro antibacterial and anthelmintic activity. The compound exhibited poor antibacterial and moderate anthelmintic activity.

Acknowledgments

The authors would like to thank Sapala organics for spectral analysis and Department of Biotechnology and Environmental Science, Tumkur University, Tumkur for the biological experiment.

Supplementary Materials

CCDC 949436 contains the supplementary crystallographic data for this paper. These data can be obtained free of charge from the Cambridge Crystallographic Data Centre, 12 Union Road, Cambridge CB2 1EZ, UK; fax: (+44) 1223 336 033; or e-mail: deposit@ccdc.cam.ac.uk.

References

- [1] Chimirri, A., Grasso, S., Molica, C., Monforte, A. M., Monforte, P., *et al.* (1996). *Il Farmaco.*, 51, 279–82.
- [2] Kemnitzer, W., Kuemmerle, J., Zhang, H. Z., Kasibhatla, S., Tseng, B., *et al.* (2009). *Bioorg. Med. Chem. Lett.*, 19, 4410–4415.
- [3] Nicolaides, D. N., Fylaktakidou, K. C., Litinas, K. E. & Hadjipavlou-Litina, D. (1998). *Eur. J. Med. Chem.*, 33, 715–724.
- [4] (a) Xu, P.-F., Zhang, Z.-H., Hui, X.-P., & Zhang, Z.-Y. (2004). *J. Chinese Chem. Soc.*, 51, 315–319. (b) Manojkumar, K. E., Sreenivasa, S., Mohan, N. R., Madhuchakrapani Rao, T., & Harikrishna, T. (2013). *J. Appl. Chem.*, 2(4), 730–737.
- [5] Reddy, G. D., Park, S.-J., Cho, H. M., Kim, T.-J., & Lee, M. E. (2012). *J. Med. Chem.*, 55, 6438–6444.
- [6] Gadegoni, H., & Manda, S. (2013). *Chinese Chem. Lett.*, 24(2), 127–130.
- [7] Singh, P., Sharma, P. K., Sharma, J. K., Upadhyay, A., & Kumar, N. (2012). *Org. Med. Chem. Lett.*, 2/8.
- [8] Manjunatha, K., Boja P., Prajwal L. L., Fernandes, J., & Suchetha Kumari, N. (2010). *Eur. J. Med. Chem.*, 45, 5225–5233.
- [9] Sanjeevarayappa, C., Pushpa Iyengar, S. T., Manoj Kumar, K. E., & Prathap, H. K. (2014). *J. Appl. Chem.*, 3(1), 38–46.
- [10] Bruker (2004). *APEX2, SAINT-Plus and SADABS*. Bruker AXS Inc., Madison, Wisconsin, USA.
- [11] Sheldrick, G. M. (2008). *Acta Cryst.*, A64, 112–122.
- [12] Allen, F. H., Kennard, O., Watson, D. G., Brammer, L., Orpen, A. G., *et al.* (1987). *J. Chem. Soc., Perkin II*, S1–S18.
- [13] Macrae, C. F., Bruno, I. J., Chisholm, J. A., Edgington, P. R., McCabe, P., *et al.* (2008). *J. Appl. Cryst.*, 41, 466–470.
- [14] Cremer, D., & Pople, J. A. (1975). *J. Am. Chem. Soc.*, 97(6), 1354–1358.
- [15] Bernstein, J., Davis, R. E., Shimon, L., & Chang, N.-L. (1995). *Angew. Chem. Int. Ed. Engl.*, 34, 1555–1573.
- [16] Droge, W. (2002). *Physiol Rev.*, 82, 47–95.
- [17] Manojkumar, K. E., Sreenivasa, S., Mohan, N. R., Aruna Kumar, D. B., Thippeswamy, B. S., *et al.* (2013). *Indo Am. J. Pharm. Res.*, 3(10), 8154–8164.
- [18] Haque, R., & Mondal, S. (2011). *Int. J. Drug Dev. Res.*, 3(4), 94–100.